지방이식의 생존을 위한 대사적 리프로그래밍

석 사 학 위 논 문

Fat Graft Survival Requires Metabolic Reprogramming Toward the Glycolytic Pathway

계 명 대 학 교 대 학 원

의 학 과

이 강 희

지도교수 조 태 희

2022년 8월

이 강 희

2022년 8월

Fat Graft Survival Requires Metabolic Reprogramming Toward the Glycolytic Pathway

지도교수 조 태 희

이 논문을 석사학위 논문으로 제출함

2022 년 8 월

계 명 대 학 교 대 학 원

의학과 성형외과학 전공

이 강 희

이강희의 석사학위 논문을 인준함

주 심 최 재 훈

부 심 정 운 혁

부 심 조 태 희

계 명 대 학 교 대 학 원

2022 년 8 월

감사의 말씀

길고도 짧았던 대학원과정도 마무리 되어가고 있습니다. 그간 코로나 시국으로 비대면 수업이 주를 이뤘고 교정에 들어간 지도 벌써 오랜 시간이 지났습니다.

하나의 논문으로 모든걸 알 수는 없지만, 하나하나의 연구가 모여 어떠한 위대한 기초를 만든다고 생각합니다. 저 또한 그 기초가 되기 위한 한 발자국이 되고 싶습니다.

본 논문을 제출하기까지 아낌없는 조언과 가르침을 주신 조태희 지도교수님께 진심으로 감사의 인사를 드립니다. 또한, 바쁘신 가운데에도 더 좋은 논문이 될 수 있도록 많은 관심을 가져주신 손대구 교수님, 김준형 교수님, 최재훈 교수님 및 정운혁 교수님께도 감사의 말씀을 드립니다.

2022년 8월

이 강 희

Table of Contents

List of Tables

List of Figures

1. Introduction

Autologous fat graft has been widely used in reconstructive and cosmetic surgery as a natural filler (1,2). It is abundant, naturally integrated into recipient sites, and has the potential to be permanent (3,4). However, despite these advantages, fat grafts are resorbed at various rates, making it difficult to predict the outcomes (5-10). Therefore, improving the graft survival rate has been the primary focus of fat graft researches. There are numerous studies investigating fat grafting methods, such as various cell-assisted lipotransfer, recipient site preconditioning methods and ideal technique for graft, which enhanced graft retention (11-18). Also, various researches have been carried out to determine fat graft survival mechanisms (5, 19, 20, 21, 22). The earliest research in fat graft survival was described by Peer. He proposed that the mechanism of fat graft survival is based on establishing early blood circulation through anastomosis of the fat graft and host blood vessels. Certain durable cells in the fat graft receive an early and adequate circulation and continue to survive, whereas the remainder of the graft degenerates and is gradually eliminated (8). On the other hands, some authors have challenged the common belief that grafted living adipocytes could survive and remain

alive for a long period. Yoshimura et al. have focused on the effects of ischemia, finding that adipocytes undergo apoptosis and necrosis as early as 24 hours after the onset of ischemia. In contrast, adipose-derived stem/progenitor cells survive for three days after onset (21, 22). Based on these findings, in vivo studies determined that only a marginal number of adipocytes survive after grafting; most adipocytes are eventually replaced with newly differentiated adipocytes from adipose-derived stromal cells (ASCs) (21). Additionally, researchers used fluorescent reporter tracing, observing that supplemented ASCs participate in angiogenesis and differentiate into adipocytes that integrate with surviving donor fat (23).

All of the aforementioned studies are feasible to have an effect on the survival of grafted adipose tissue. However, those studies focused on secondary issues, such as recipient's environment or grafting methods, rather than grafted fat itself. Also, mechanistic studies were primarily limited to histological and morphological analyses, and the fundamental molecular mechanisms underlying non-vascularized fat graft survival are not entirely understood. Therefore, we performed an unbiased transcriptomic analysis and subsequent pharmacological study of a mouse free fat graft model to determine the molecular mechanisms underlying free fat graft survival.

2. Material and Methods

Mouse fat graft model

Animal studies were performed following the protocols (KM-2021-31) approved by the Animal Care Committee for Animal Research of Keimyung University. Specific pathogen-free 8-week-old C57BL/6J male mice (Charles River Laboratories Japan, Kanagawa, Japan) were maintained at room temperature (21 to 25 ° C) and fed a standard chow diet and tap water ad libitum. All mice underwent anesthesia via isoflurane inhalation before the surgical and sampling procedures. The left subcutaneous inguinal adipose tissue was harvested en bloc through a midline abdominal incision for the autologous mouse fat graft model (Fig. 1A and B). The weight of the harvested adipose tissue was recorded for each mouse, and then the tissue was grafted at the harvest site without any tissue modifications. The right contralateral subcutaneous inguinal adipose tissue was used as a non-graft control (Fig. 2A).

Fat graft RNA extraction

Grafted adipose tissues were harvested on days 3 and 7 after grafting (Graft group, n = 5). Contralateral adipose tissues were harvested and

used as controls (Control group, n = 5). Each specimen was weighed and immediately frozen in liquid nitrogen. The samples were then homogenized with an appropriate volume of TRIzol reagent (Invitrogen, Carlsbad, CA, USA) in independent, safe lock tubes containing beads. After triazole/chloroform extraction, the aqueous phase was mixed with 100 % ethanol and loaded onto an RNeasy column (Qiagen, Valencia, CA, USA). RNA extraction was performed according to the manufacturer's protocol.

RNA-sequencing (RNA-seq) data analysis

Libraries were prepared for 151-bp paired-end sequencing using the TruSeq stranded messenger RNA (mRNA) Sample Preparation Kit (Illumina, San Diego, CA, USA). mRNA molecules were purified and fragmented from 1 μg of total RNA using oligo (dT) magnetic beads. Fragmented mRNAs were synthesized as single-stranded complementary DNAs (cDNAs) through random hexamer priming and then used as templates for double-stranded cDNA synthesis. After sequential end repair, A-tailing, and adapter ligation, the cDNA libraries were amplified by polymerase chain reaction. The quality of these cDNA libraries was evaluated using an Agilent 2100 BioAnalyzer (Agilent, Santa Clara, CA, USA); the libraries were quantified using the KAPA Library Quantification Kit (Kapa

Biosystems, Wilmington, MA, USA) per the manufacturer's library quantification protocol. After cluster amplification of the denatured templates, paired-end sequencing (2 × 151 bp) was performed using Illumina NovaSeq6000 (Illumina, USA). The adapter sequences and read ends with Phred quality scores less than 20 were trimmed; reads shorter than 50 bp were removed simultaneously using Cutadapt v.2.8.(24) Filtered reads were mapped to the reference genome related to the species using the aligner STAR v.2.7.1a following ENCODE standard options with the "-quantMode TranscriptomeSAM" option to estimate transcriptome expression levels.(25) Gene expression was estimated using RSEM v.1.3.1.(26) Next, transcript per million (TPM) values were calculated to normalize the sequencing depth among samples. Then, the TPM values were processed for principal component analysis (PCA) and unsupervised hierarchically clustered heat map generation. Next, a gene set enrichment analysis (GSEA) was performed with hallmark gene set collections of the Molecular Signature Database v7.4.(27) False discovery rate (FDR) q-values <0.15 were considered statistically significant.

Pharmacological study with histological staining

We used the same mouse fat graft model described above to regulate

metabolic pathways in grafted fat. Left inguinal fat was harvested, weighed, and grafted in situ for each mouse. Once every two days, 2-Deoxy-D-glucose (2-DG; 500 mg/kg of body weight, Sigma-Aldrich, Saint Louis, MO, USA) in phosphate-buffered saline (PBS; 100μL) and 20% glucose (1g/kg of body weight, Choongwae, Seoul, Republic of Korea) were injected in grafted fat (2-DG group; n = 5, Glucose group; n = 5). PBS (100μL) alone was used as the control (PBS group; n = 5) (Fig. 2B). The mouse body weights were tracked to determine whether the drug had any whole-body effect during the injection course. After 15 time injections, the grafted fats were harvested and weighed in all group for retention rate comparisons. In addition, contralateral right inguinal fat weight was measured to observe any nonspecific adipose effects of the drug injection.

For histologic analysis, harvested adipose tissues were fixed overnight with a 10 % neutral buffered formalin solution (Sigma-Aldrich) at 4 ° C. After paraffin embedding, 5 μm sections were prepared for hematoxylin and eosin (H&E) staining. For immunofluorescence staining, rehydrated sections were blocked with 10 % goat serum in 1 % bovine serum albumin and then incubated at 4 ° C overnight with a rabbit anti-mouse perilipin antibody (1:1000, #3470, Cell Signaling Technology, Beverly, MA, USA). After several washes, the samples were incubated for 2 hours at room temperature with Alexa Fluor 594-conjugated anti-rabbit

IgG (ab150080, Abcam, United Kingdom). Then, the samples were mounted with Prolong Gold antifade reagent with DAPI (Invitrogen, USA), and immunofluorescent images were acquired using an Axiovert 200M microscope (Zeiss, Oberkochen, Germany).

Statistical analyses

Data are presented as means ± standard errors of the mean (SEMs). Statistical differences were compared using a two-tailed, unpaired *t*-tes and one-way analysis of variance (ANOVA). Differences with a value of $p < 0.05$ was considered statistically significant.

3. Results

Grafted adipose tissues have differentially expressed gene profiles

Prior to RNA-seq, the weights of adipose tissue were analysed. In the graft group, the weights of adipose tissue were significantly increased, compared to the contralateral control in both 3-and 7-day ($p < 0.05$) (Table 1, Fig. 3). When compared with the weights before grafting, the adipose tissues demonstrated weight increase after grafting, although the statistics were not significant. The change we observed before and after the grafting may owe to the direct edematous and inflammatory stimulus of fat graft surgery. However, the significant weight reduction of the contralateral adipose tissues may be the result of whole body surgical stress by general anesthesia.

Total fifteen adipose tissue samples were subjected to RNA-seq, including (1) contralateral control adipose tissue (n = 5), (2) 3-day graft (n = 5), and (3) 7-day graft (n = 5). The PCA plot, which demonstrates sample clustering based on similarity, illustrated global differences in the transcriptomes of the grafted fat and the control (Fig. 4A). The 3-and 7-day graft transcriptomes was exhibited quite similar and clustered with each other. The heatmap also demonstrated hierarchical clustering of the transcriptomes of these samples (Fig.

4B). Furthermore, the PCA and heatmap results demonstrated that the transcriptome changes from grafting were biologically consistent, supporting further transcriptomic analyses.

Grafted adipose tissues undergo a metabolic shift from fatty acid metabolism to glycolysis

GSEA, a knowledge-based gene set analysis, identified biologically meaningful gene expression differences among the study groups. We analyzed the transcriptomes of the 3-and 7-day grafts by comparing them with those of the control non-graft adipose tissue. As a result, gene sets related to the epithelial-mesenchymal transition (FDR: q = 0.005) and hypoxia (FDR: q = 0.01) were the most upregulated in the 3-day grafts compared to those in the control grafts (Fig. 5A). Genes sets related to tumor necrosis factor-alpha (i.e., TNF-α) signaling via nuclear factor-kappa B (i.e., NFκB) (FDR: q = 0.022), the reactive oxygen species pathway (FDR: q = 0.028), complement (FDR: q = 0.026), inflammatory response (FDR: q = 0.024), and interleukin 6 Janus kinase-signal transducer and activator of transcription (i.e., JAK-STAT) signaling (FDR: q = 0.029), which are primarily inflammation-related pathways, were also significantly upregulated in the 3-day grafts. In the 7-day grafts, genes sets related to angiogenesis (FDR: q = 0.023)

were the most upregulated compared to those in the control grafts; genes sets related to inflammation-related pathways, including complement (FDR: q = 0.092) and inflammatory response (FDR: q = 0.088), were also upregulated (Fig. 5B).

Mechanistically, the glycolytic pathway was upregulated in the 3-day (FDR: q = 0.012) and 7-day (FDR: q = 0.084) fat grafts. In contrast, the top and most commonly upregulated gene sets in the control fat compared with those in the grafted fat were fatty acid metabolism (3-day graft FDR: q = 0.028; 7-day graft FDR: q = 0.125) and adipogenesis (3-day graft FDR: q = 0.084; 7-day graft FDR: q = 0.062) (Fig. 6A and B). Together, these results demonstrate that the grafted adipose tissues undergo transcriptomic shift from fatty acid metabolism to glycolysis.

Glycolysis regulation in fat grafts affects graft retention rates

Next, to find out the effects of glycolysis pathway in fat graft retentions, we injected glucose and 2-DG directly to fat grafts in mouse model (Fig. 7). The PBS, glucose and 2-DG groups (n = 5 per group) had comparable weight gain during the 4-week injection period, suggesting that the localized drug injection did not affect whole-body metabolism (Fig. 8A). There were no significant differences of mouse

weight between three groups at the point of tissue harvest (Fig. 8B). The weights of adipose tissue were comparable between three groups. The only significant difference was observed in the 2-DG group. The weights of grafted adipose tissue was reduced after 4 week 2-DG injection following grafting when compared with the PBS control (Table 2, Fig. 9). In contrast, the volume increase observed in the glucose group was not statistically significant. In the macroscopic comparison of the adipose tissue, the volumes of grafted adipose tissue were reduced in 2-DG group when compared with the PBS group (Fig. 10). Of note, the right contralateral control weight did not differ between three groups upon harvest after 4 weeks of injections, indicating that localized injections did not affect whole-body adipose metabolism (Fig. 9).

Glycolysis inhibition in fat grafts reduces marginal adipocyte survival

To microscopically visualize the reduced fat graft volume in the 2-DG group, we performed H&E and perilipin staining. In H&E staining, the 2-DG group demonstrated more widespread fibrosis and higher number of lipid vacuoles with seemingly low viability when compared with the PBS group (Fig. 11, above). The PBS group had large perilipin-unstained lobules and small perilipin-stained adipocytes, implying active death and adipocyte regeneration. In contrast, the 2-DG group exhibited

relatively unevenly sized fat cells with perilipin-negative surroundings (Fig. 11, below). These results suggested that the glycolysis suppression in fat grafts interrupts the dynamic adipose remodeling process, more specifically, the marginal adipose regeneration of fat grafts.

4. Discussion

The mechanical manipulation of fat grafting process is likely to result in various biochemical, molecular and microenvironmental changes of adipose tissues. However, The specific mechanisms related to survival of fat grafts are still unknown. In this study, we performed a transcriptomic analysis of mouse free fat graft model to find out the molecular changes in unbiased manner.

Previously, Schreiter et al. performed a microarray analysis of 7-day and 15-day subcutaneous fat grafts in female C57BL/6N mice. Using a differentially expressed gene analysis, they found that the genes related to extracellular matrix remodeling and inflammation were upregulated, while lipid metabolism-related genes were downregulated after transplantation (28). In this study, we performed RNA-seq, which detects a higher percentage of differentially expressed genes and a larger dynamic range than the array technology (29-34). Moreover, we searched for more direct mechanisms that may affect the survival and retention rates of fat grafts, to further translate molecular research to clinics.

Based on previous observations by Suga et al., we chose to analyze the transcriptome on days 3 and 7 after grafting, when ischemic and

angiogenic/adipogenic effects are expected to be highly active, respectively (22). We used solely male mice in order to exclude any effects of sex hormones on adipose metabolism. Moreover, we did not manipulate the adipose tissues to prevent the effects of mechanical stimuli on gene expression.(35, 36) As other studies identified that changing the location of adipose tissue leads to change type of adipose tissue or even overall metabolism of whole body, we did not change the adipose tissue location for fat grafting. Instead, we grafted them in situ to exclude depot-and location-specific effects of adipose tissues (37-39).

We attempted to minimize adipose tissue handling before grafting in our experiments; thus, we did not break down the fat, trying to minimize additional effects from mechanical stimuli. We also considered that artificial ex vivo fat fragmentation does not precisely resemble fat dissociation during human fat harvesting. However, our model did contain a disadvantageous large fat volume for grafting, which may appear as large fat necrosis in the core of the graft. To minimize any effects of necrosis on RNA quality, we chose to extract RNA in the Trizol-containing bead-beating tubes that break down the specimens from the periphery. We also performed RNA extraction by adding an additional centrifugation step before phenol-chloroform extraction to minimize the effects of contamination.

Our PCA plot and heatmap analysis suggest significant changes by showing consistent and clustered transcriptome differences between fat grafts and control adipose tissues, suggesting significant changes. In GSEA, we performed GSEA with hallmark gene set collections to acquire biological insights into transcriptome changes (27). The 3-day grafts demonstrated significantly increased expression of hypoxia-and inflammation-related genes, whereas the 7-day grafts exhibited upregulation of angiogenesis-related genes. It is well-known that hypoxic state must follow after non-vascularized fat graft (40-43). And fat graft induces inflammation through activation of pro-inflammatory cytokines in adipose tissue due to hypoxia (44). Our consistent molecular observations with previous studies can enhance the reliability of our results.

Adipose tissue consists of adipocytes, ASCs, vascular endothelial cells, pericytes, fibroblasts, macrophages and extracellular matrix (45). In general, cells and tissues predominantly consume glucose and fatty acids for survival and adaptation (46-48). To identify potential graft survival mechanisms, we focused on the glycolytic pathway, which was upregulated metabolic pathway in both 3-and 7-day grafts. In addition, we found that the control fat had more upregulation of fatty acid metabolism-related genes than the 3-and 7-day grafted fats. These results indicate that fat grafts undergo a metabolic shift from fatty

acid-dominant metabolism to glycolysis-dominant metabolism.

To determine the effect of the glycolysis shift on graft survival, we performed a pharmacological regulation study in a mouse fat graft model. We found that 4-week localized suppression of glycolysis in the fat grafts significantly reduced the graft retention rate, possibly by suppressing marginal adipose survival and regeneration. Conversely, the amplification through local glucose injection showed an increase in volume, although the results were not statistically significant. Histologically, we found the viable adipocytes was significantly decreased in pharmacological inhibition groups. We also tracked the whole-body weight and checked the contralateral inguinal fat mass, ruling out whole-body drug effects. Therefore, we could conclude that adipose tissues undergo a metabolic shift to glycolysis for survival after non-vascularized grafting.

Previous studies have suggested a shift to glycolysis in fat grafts. For example, a 2010 study by Suga et al. describing the phenomenon of adipose ischemia demonstrated that fats increase fibroblast growth factor-2 (FGF-2) expression in response to ischemia (22). It is widely assumed that the primary function of a growth factor is to regulate glucose uptake and metabolism, thus maintaining mitochondrial homeostasis and activating anabolic pathways required for cell growth. Growth factors also critically regulate glucose uptake and glycolysis-

related genes, implying that increased FGF-2 expression in adipose ischemia may be related to the glycolysis increase in our fat graft model (49). Our study adds to this finding that underlying transcriptome changes to the glycolytic pathway may contribute to higher glucose metabolism after fat grafting.

Taking a closer look to the results of glucose injections in fat grafts, we need deeper discussion about the glycolysis. Glycolysis is a basic energy metabolism process carried out even in prokaryotes (50). In anaerobic conditions, as in the fat grafts, the cells predominantly produce ATP by glycolysis and reduces the portions produced by oxidative phosphorylations. In specific conditions, when the glycolysis process has to occur continuously, NAD+ is depleted and eventually the glycolysis process is stopped (51). Because of this, most tissues do not withstand the anaerobic conditions for a long time and are destroyed. Glycolysis is stopped without NADH oxidation process, and consequently, it is stopped no matter how much glucose is present. The amounts of enzymes are limited for every conditions, so we had to consider that the simple glucose injections in our model may have not led to glycolysis increase in the fat grafts. Taken together, we could conclude that it may be inappropriate to consider that glucose local injection amplified the glycolysis pathway. However, the ischemic state after non-vascularized fat graft is inevitable, and to ideally concretize our

study scheme to increase glycolysis in fat grafts, we need more delicate study designs. In a recent study, NADH oxidase, which oxidizes NADH to NAD+, was obtained from lactobacillus (52). If this is continuously injected with glucose, it may be possible to produce energy withstanding in the ischemic state.

In the Warburg effect first described in the 1920s (53), the cancer cells generate energy via glycolysis rather than mitochondrial oxidative phosphorylation even in the presence of oxygen. Although the glycolytic shift observed in our fat graft model may have resulted from obvious ischemic conditions, we still must consider that more fundamental metabolic reprogramming may occur after non-vascularized adipose tissue grafting. Future studies will focus on the identification of up-stream molecular pathways, and the translation of our findings in clinics.

References

1. Billings, E., Jr., May, J. W., Jr. Historical review and present status of free fat graft autotransplantation in plastic and reconstructive surgery. Plast Reconstr Surg 1989;83:368-381.
2. Pu, L. L., Yoshimura, K., Coleman, S. R. Future Perspectives of Fat Grafting. Clin Plast Surg 2015;42:389-394, ix-x.
3. Clauser, L. C., Tieghi, R., Galiè, M., Carinci, F. Structural fat grafting: facial volumetric restoration in complex reconstructive surgery. J Craniofac Surg 2011;22:1695-1701.
4. Coleman, S. R. Structural fat grafting: more than a permanent filler. Plast Reconstr Surg 2006;118:108s-120s.
5. Doornaert, M., Colle, J., De Maere, E., Declercq, H., Blondeel, P. Autologous fat grafting: Latest insights. Ann Med Surg (Lond) 2019;37:47-53.
6. Zheng, H., Yu, Z., Deng, M., et al. Fat extract improves fat graft survival via proangiogenic, anti-apoptotic and pro-proliferative activities. Stem Cell Res Ther 2019;10:174.
7. Zhu, M., Cohen, S. R., Hicok, K. C., et al. Comparison of three

different fat graft preparation methods: gravity separation, centrifugation, and simultaneous washing with filtration in a closed system. Plast Reconstr Surg 2013;131:873-880.

8. Peer, L. A. Loss of weight and volume in human fat grafts: with postulation of a "cell survival theory". Plastic and reconstructive surgery 1950;5:217-230.

9. Coleman, S. R. Structural fat grafts: the ideal filler? Clin Plast Surg 2001;28:111-119.

10. Kaufman, M. R., Miller, T. A., Huang, C., et al. Autologous fat transfer for facial recontouring: is there science behind the art? Plast Reconstr Surg 2007;119:2287-2296.

11. Paik, K. J., Zielins, E. R., Atashroo, D. A., et al. Studies in Fat Grafting: Part V. Cell-Assisted Lipotransfer to Enhance Fat Graft Retention Is Dose Dependent. Plast Reconstr Surg 2015;136:67-75.

12. Rasmussen, B. S., Sørensen, C. L., Kurbegovic, S., et al. Cell-Enriched Fat Grafting Improves Graft Retention in a Porcine Model: A Dose-Response Study of Adipose-Derived Stem Cells versus Stromal Vascular Fraction. Plast Reconstr Surg 2019;144:397e-408e.

13. Yu, F., Witman, N., Yan, D., et al. Human adipose-derived stem cells enriched with VEGF-modified mRNA promote angiogenesis and long-term graft survival in a fat graft transplantation model. Stem Cell Res Ther 2020;11:490.

14. Eto, H., Suga, H., Inoue, K., et al. Adipose injury-associated factors mitigate hypoxia in ischemic tissues through activation of adipose-derived stem/progenitor/stromal cells and induction of angiogenesis. Am J Pathol 2011;178:2322-2332.

15. Fu, S., Luan, J., Xin, M., Wang, Q., Xiao, R., Gao, Y. Fate of adipose-derived stromal vascular fraction cells after co-implantation with fat grafts: evidence of cell survival and differentiation in ischemic adipose tissue. Plast Reconstr Surg 2013;132:363-373.

16. Kim, J., Park, M., Jeong, W., et al. Recipient-Site Preconditioning with Deferoxamine Increases Fat Graft Survival by Inducing VEGF and Neovascularization in a Rat Model. Plast Reconstr Surg 2019;144:619e-629e.

17. Lin, J. Y., Wang, C., Pu, L. L. Can we standardize the techniques for fat grafting? Clin Plast Surg 2015;42:199-208.

18. Pu, L. L. Towards more rationalized approach to autologous fat

grafting. J Plast Reconstr Aesthet Surg 2012;65:413-419.

19. Pu, L. L. Mechanisms of Fat Graft Survival. Ann Plast Surg 2016;77 Suppl 1:S84-86.

20. Evans, B. G. A., Gronet, E. M., Saint-Cyr, M. H. How Fat Grafting Works. Plast Reconstr Surg Glob Open 2020;8:e2705.

21. Eto, H., Kato, H., Suga, H., et al. The fate of adipocytes after nonvascularized fat grafting: evidence of early death and replacement of adipocytes. Plast Reconstr Surg 2012;129:1081-1092.

22. Suga, H., Eto, H., Aoi, N., et al. Adipose tissue remodeling under ischemia: death of adipocytes and activation of stem/progenitor cells. Plast Reconstr Surg 2010;126:1911-1923.

23. Hong, K. Y., Yim, S., Kim, H. J., et al. The Fate of the Adipose-Derived Stromal Cells during Angiogenesis and Adipogenesis after Cell-Assisted Lipotransfer. Plast Reconstr Surg 2018;141:365-375.

24. Martin, M. Cutadapt removes adapter sequences from high-throughput sequencing reads. EMBnet journal 2011;17:10-12.

25. Dobin, A., Davis, C. A., Schlesinger, F., et al. STAR: ultrafast universal RNA-seq aligner. Bioinformatics 2013;29:15-21.

26. Li, B., Dewey, C. N. RSEM: accurate transcript quantification from RNA-Seq data with or without a reference genome. BMC Bioinformatics 2011;12:323.

27. Subramanian, A., Tamayo, P., Mootha, V. K., et al. Gene set enrichment analysis: a knowledge-based approach for interpreting genome-wide expression profiles. Proc Natl Acad Sci U S A 2005;102:15545-15550.

28. Schreiter, J. S., Kurow, L. O., Langer, S., Steinert, M., Massier, L. Effects of non-vascularized adipose tissue transplantation on its genetic profile. Adipocyte 2021;10:131-141.

29. Wang, Z., Gerstein, M., Snyder, M. RNA-Seq: a revolutionary tool for transcriptomics. Nat Rev Genet 2009;10:57-63.

30. Wilhelm, B. T., Landry, J. R. RNA-Seq-quantitative measurement of expression through massively parallel RNA-sequencing. Methods 2009;48:249-257.

31. Zhao, S., Fung-Leung, W. P., Bittner, A., Ngo, K., Liu, X. Comparison of RNA-Seq and microarray in transcriptome profiling of activated T cells. PLoS One 2014;9:e78644.

32. Wang, C., Gong, B., Bushel, P. R., et al. The concordance between

RNA-seq and microarray data depends on chemical treatment and transcript abundance. Nat Biotechnol 2014;32:926-932.

33. Li, J., Hou, R., Niu, X., et al. Comparison of microarray and RNA-Seq analysis of mRNA expression in dermal mesenchymal stem cells. Biotechnol Lett 2016;38:33-41.

34. Liu, Y., Morley, M., Brandimarto, J., et al. RNA-Seq identifies novel myocardial gene expression signatures of heart failure. Genomics 2015;105:83-89.

35. Lundholm, L., Putnik, M., Otsuki, M., et al. Effects of estrogen on gene expression profiles in mouse hypothalamus and white adipose tissue: target genes include glutathione peroxidase 3 and cell death-inducing DNA fragmentation factor, alpha-subunit-like effector A. J Endocrinol 2008;196:547-557.

36. Marques, M. A., Combes, M., Roussel, B., et al. Impact of a mechanical massage on gene expression profile and lipid mobilization in female gluteofemoral adipose tissue. Obes Facts 2011;4:121-129.

37. Tran, T. T., Yamamoto, Y., Gesta, S., Kahn, C. R. Beneficial effects of subcutaneous fat transplantation on metabolism. Cell Metab 2008;7:410-420.

38. Satoor, S. N., Puranik, A. S., Kumar, S., et al. Location, location, location: Beneficial effects of autologous fat transplantation. Sci Rep 2011;1:81.

39. Hoppela, E., Grönroos, T. J., Saarikko, A. M., et al. Fat Grafting Can Induce Browning of White Adipose Tissue. Plast Reconstr Surg Glob Open 2018;6:e1804.

40. Baran, C. N., Celebioğlu, S., Sensöz, O., Ulusoy, G., Civelek, B., Ortak, T. The behavior of fat grafts in recipient areas with enhanced vascularity. Plast Reconstr Surg 2002;109:1646-1651; 1652.

41. Brucker, M., Sati, S., Spangenberger, A., Weinzweig, J. Long-term fate of transplanted autologous fat in a novel rabbit facial model. Plast Reconstr Surg 2008;122:749-754.

42. Coban, Y. K., Ciralik, H. The effects of increased ischemic times on adipose tissue: a histopathologic study using the epigastric flap model in rats. Aesthetic Plast Surg 2007;31:570-573.

43. Zhong, X., Yan, W., He, X., Ni, Y. Improved fat graft viability by delayed fat flap with ischaemic pretreatment. J Plast Reconstr Aesthet Surg 2009;62:526-531.

44. Ye, J., Gao, Z., Yin, J., He, Q. Hypoxia is a potential risk factor for chronic inflammation and adiponectin reduction in adipose tissue of ob/ob and dietary obese mice. Am J Physiol Endocrinol Metab 2007;293:E1118-1128.

45. Yoshimura, K., Shigeura, T., Matsumoto, D., et al. Characterization of freshly isolated and cultured cells derived from the fatty and fluid portions of liposuction aspirates. J Cell Physiol 2006;208:64-76.

46. Krishna, M. S., Revathy, V. M., Jaleel, A. Adipocytes utilize sucrose as an energy source-Effect of different carbohydrates on adipocyte differentiation. J Cell Physiol 2020;235:891-899.

47. Morigny, P., Boucher, J., Arner, P., Langin, D. Lipid and glucose metabolism in white adipocytes: pathways, dysfunction and therapeutics. Nat Rev Endocrinol 2021;17:276-295.

48. Yoshimura, K., Suga, H., Eto, H. Adipose-derived stem/progenitor cells: roles in adipose tissue remodeling and potential use for soft tissue augmentation. Regen Med 2009;4:265-273.

49. Vander Heiden, M. G., Plas, D. R., Rathmell, J. C., Fox, C. J., Harris, M. H., Thompson, C. B. Growth factors can influence cell growth and survival through effects on glucose metabolism. Mol

Cell Biol 2001;21:5899-5912.

50. Romano, A. H., Conway, T. Evolution of carbohydrate metabolic pathways. Res Microbiol 1996;147:448-455.

51. Hopp, A. K., Grüter, P., Hottiger, M. O. Regulation of Glucose Metabolism by NAD(+) and ADP-Ribosylation. Cells 2019;8.

52. Nowak, C., Beer, B., Pick, A., Roth, T., Lommes, P., Sieber, V. A water-forming NADH oxidase from Lactobacillus pentosus suitable for the regeneration of synthetic biomimetic cofactors. Front Microbiol 2015;6:957.

53. Warburg, O., Wind, F., Negelein, E. THE METABOLISM OF TUMORS IN THE BODY. J Gen Physiol 1927;8:519-530.

Fat Graft Survival Requires Metabolic Reprogramming Toward the Glycolytic Pathway

Lee, Kang Hee

Department of Plastic Surgery

Graduate School

Keimyung University

(Supervised by Professor Jo, Tae Hee)

(Abstract)

Fat grafts are commonly used as natural fillers in reconstructive and cosmetic surgeries. However, the mechanisms underlying fat graft survival are poorly understood. Here, we performed an unbiased transcriptomic analysis in a mouse fat graft model to determine the underlying molecular mechanisms of free fat graft survival.

We conducted an RNA-sequencing analysis in a mouse free subcutaneous fat graft model on days 3 and 7 after grafting (n = 5). High-throughput sequencing was performed on paired-end reads using NovaSeq6000. The

transcript per million values was processed for principal component analysis (PCA), unsupervised hierarchically clustered heat map generation, and a gene set enrichment analysis.

The PCA and heat maps identified global differences between the fat graft model and the non-grafted control transcriptomes. Mechanistically, the glycolytic pathway was upregulated in the fat graft model on days 3 (false discovery rate [FDR]: q = 0.012) and 7 (FDR: q = 0.084). In subsequent experiments, pharmacological inhibition of the glycolytic pathway with 2-deoxy-D-glucose (2-DG) in the fat graft model significantly suppressed fat graft retention rates grossly and microscopically (n = 5).

Free adipose tissue grafts undergo metabolic reprogramming toward the glycolytic pathway. Future studies should examine whether targeting this pathway enhances the graft survival rate.

지방이식의 생존을 위한 대사적 리프로그래밍

이 강 희

계명대학교 대학원

의학과 성형외과학 전공

(지도교수 조 태 희)

(초록)

자가 지방 이식은 미용 및 재건 수술에서 결손을 채우기 위한 천연 필러로 많이 사용된다. 하지만, 지방 이식이 어떻게 살아남는지에 대한 메커니즘은 아직 명백히 밝혀진 바가 없다. 우리는 자가 지방 이식 생존의 분자적 메커니즘을 확인하기 위해 마우스 모델에서 비편향적인 전사체 분석을 시행하였다.

마우스의 피하지방층에 자가 지방을 이식하고 3일과 7일 뒤, 이를 채취하여 RNA 시퀀싱을 시행하였다. NovaSeq6000을 이용하여 대용량 시퀀싱을 시행하였고, TPM(transcript per million)으로 정규화 후 주성분 분석, 히트맵, GSEA(gene set enrichment analysis)을 이용하여 데이터를 분석하였다.

주성분분석과 히트맵 결과, 이식측과 비이식측간의 전반적인 차이를 보였다. GSEA에서 이식측에서 비이식측에 비해 해당 과정이 유의미하게 상향 조절

되어있었다. 이어서 시행한 약물실험에서, 2-Deoxy-D-glucose로 해당과정을 억제한 이식 편의 생존이 유의하게 억제된 것으로 나타났다.

따라서, 자가 지방 이식은 이식 후 해당과정으로의 대사적 리프로그래밍을 겪는다는 사실을 밝혀냈고, 이 과정을 이용하여 지방 이식의 생존율을 높이는 것에 대한 추가적인 연구가 필요할 것으로 생각한다.

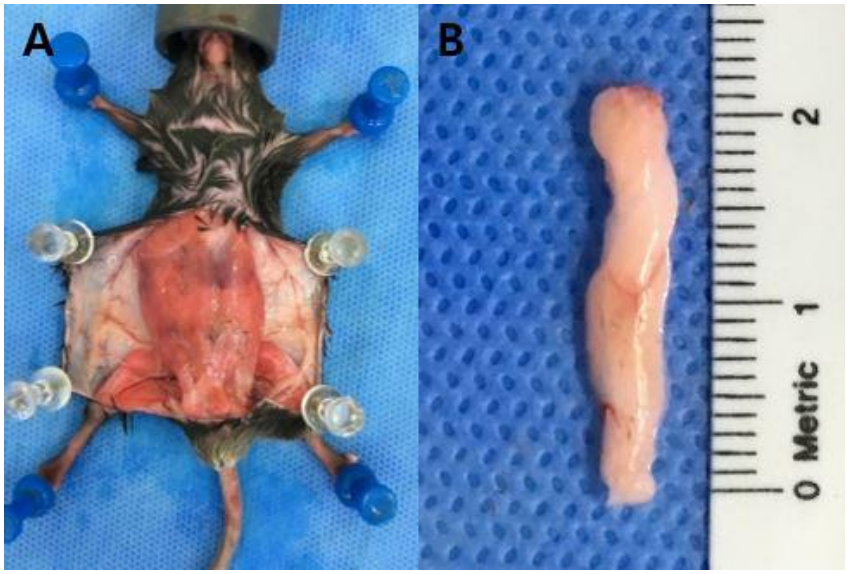

Figure 1. Mouse autologous free fat graft models were used. (A) Inguinal adipose tissue was harvested at left side with a 1.5-cm midline incision at abdomen. (B) About 100mg inguinal adipose tissue was harvested.

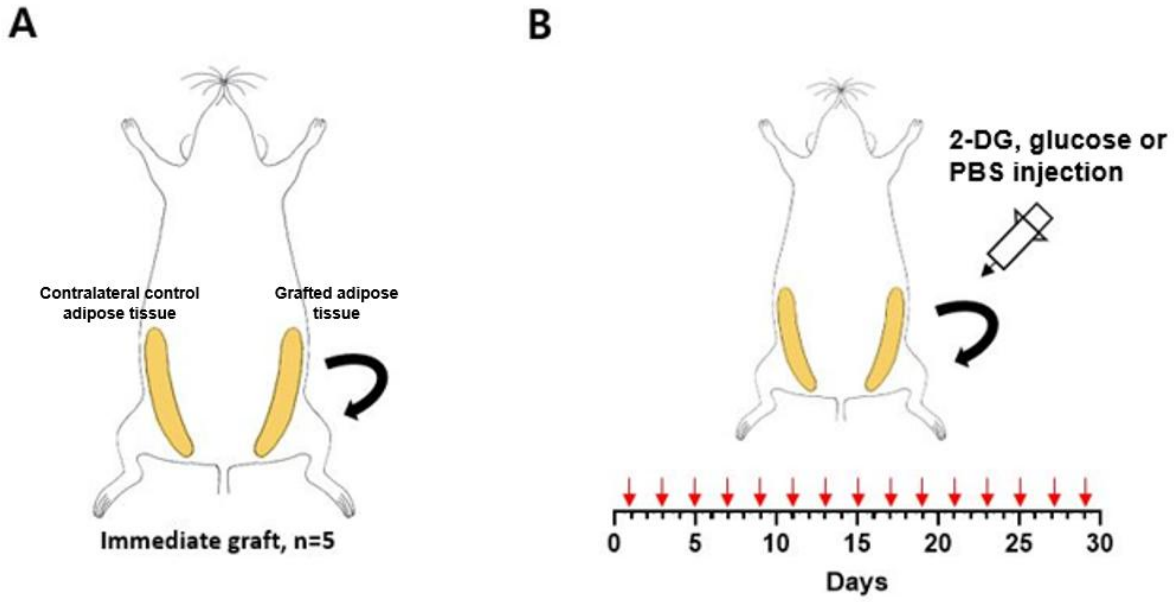

Figure 2. Experimental schematics shows how fat graft and local injection were done. (A) A schematic for comparative transcriptomic analysis of free fat grafts. Left inguinal adipose tissues were grafted in situ and compared with the right inguinal adipose tissues on days 3 and 7 after grafting. (B) A schematic for 4-week 2-Deoxy-D-glucose (2-DG) and glucose injections in a mouse fat graft model. Phosphate-buffered saline (PBS) injections were used as the control.

3-day	1	2	3	4	5
Control group	0.100	0.096	0.089	0.092	0.069
Graft group (After grafting)	0.111	0.103	0.111	0.143	0.133
Graft group (Before Grafting)	0.092	0.093	0.099	0.117	0.118

7-day	6	7	8	9	10
Control group	0.090	0.090	0.102	0.085	0.082
Graft group (After grafting) (	0.120	0.137	0.156	0.108	0.113
Graft group (Before Grafting)	0.107	0.102	0.119	0.100	0.130

Table 1. Weights of adipose tissue in each group at 3-and 7-day after grafting. Weights shown in grams (g).

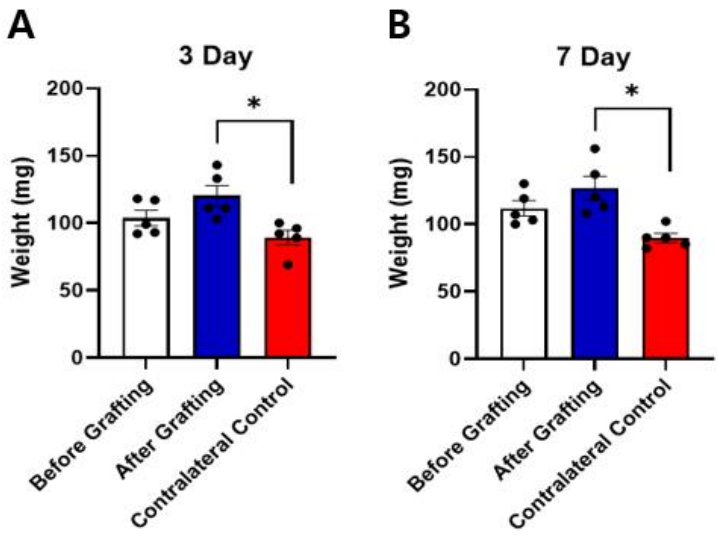

Figure 3. Weights of adipose tissue after 3-and 7-day grafting were significantly increased. (A) 3-day after graft (B) 7-day after graft. $*p < 0.05$ between indicated group. Data are presented as means ± standard errors of the mean.

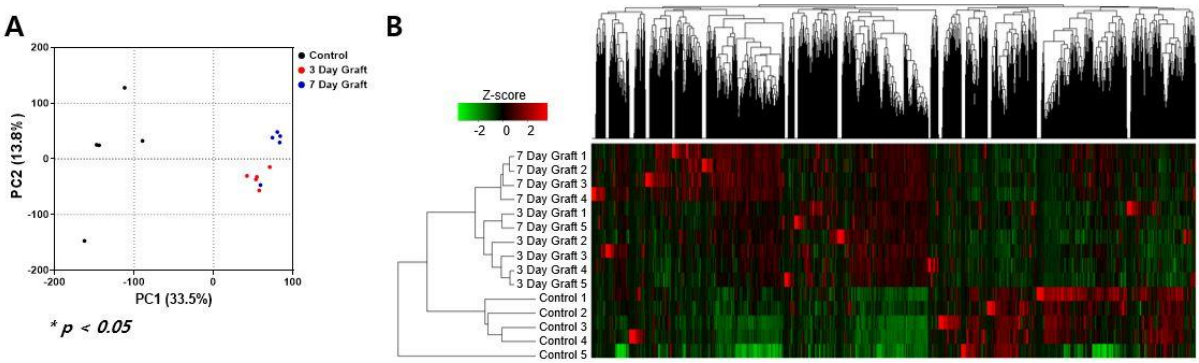

Figure 4. Non-vascularized fat grafts demonstrate distinctive transcriptomic patterns. (A) Principal component analysis(PCA) of the RNA-sequencing data from control, 3-day, and 7-day grafts (n = 5 per group), which describes 33.5% and 13.8% of the variability within the expression data set and shows global difference between two groups. (B) Free fat graft RNA-sequencing data heat maps show distinctive gene expression patterns compared with those of the control adipose tissues. The z-score scale bar represents relative expression ±2 SD from the mean.

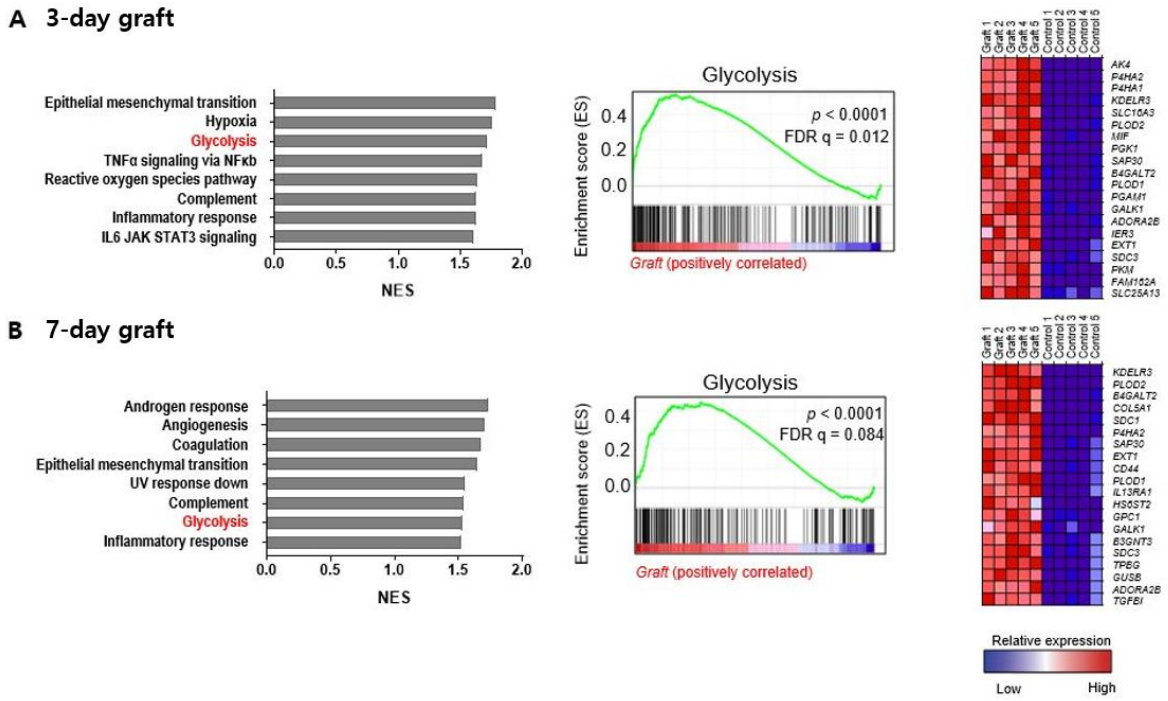

Figure 5. Non-vascularized fat grafts show transcriptional induction of glycolysis-related genes. Gene set enrichment analysis (GSEA) and heat maps of the top 20 upregulated genes for glycolysis on both day 3 (A) and day 7 (B). TNF-α, tumor necrosis factor α; NFκb, nuclear factor κb; IL-6, interleukin 6; JAK-STAT, Janus kinase-signal transducer and activator of transcription; UV, ultraviolet; NES, normalized enrichment score; FDR, false discovery rate.

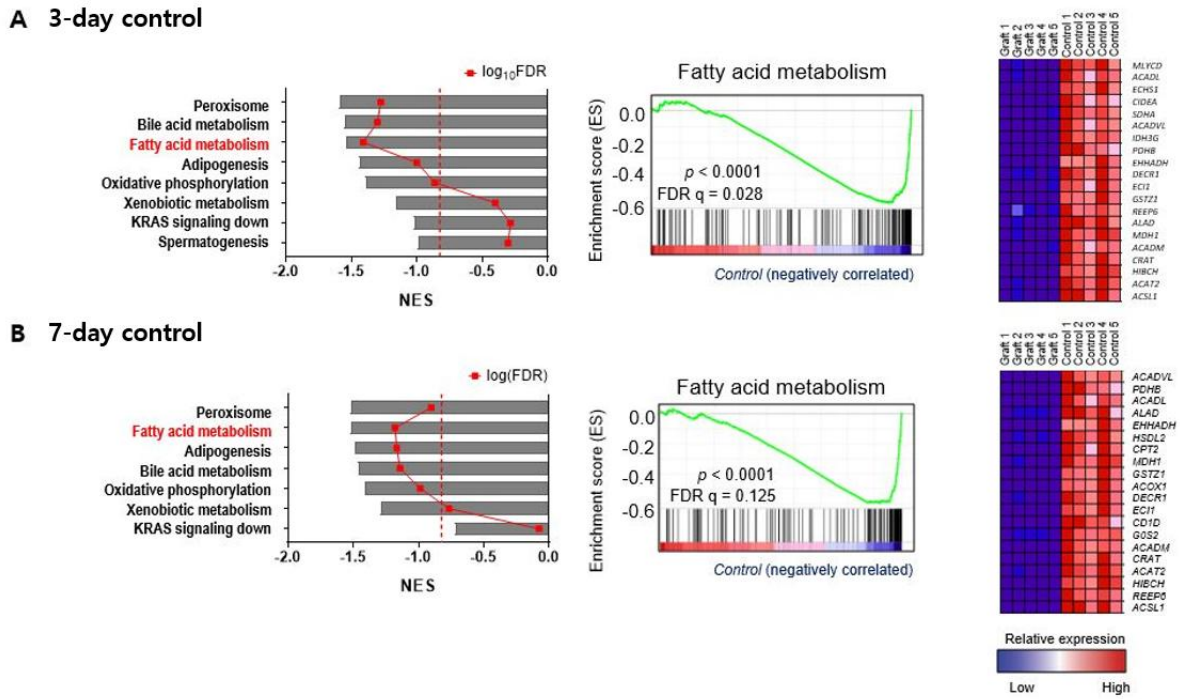

Figure 6. Control adipose tissues show upregulation of fatty acid metabolism-related genes. Gene set enrichment analysis (GSEA) results and heat maps of the top 20 upregulated genes for fatty acid metabolism in control fat compared with those of 3-day (A) and 7-day (B) grafts. NES, normalized enrichment score; FDR, false discovery rate.

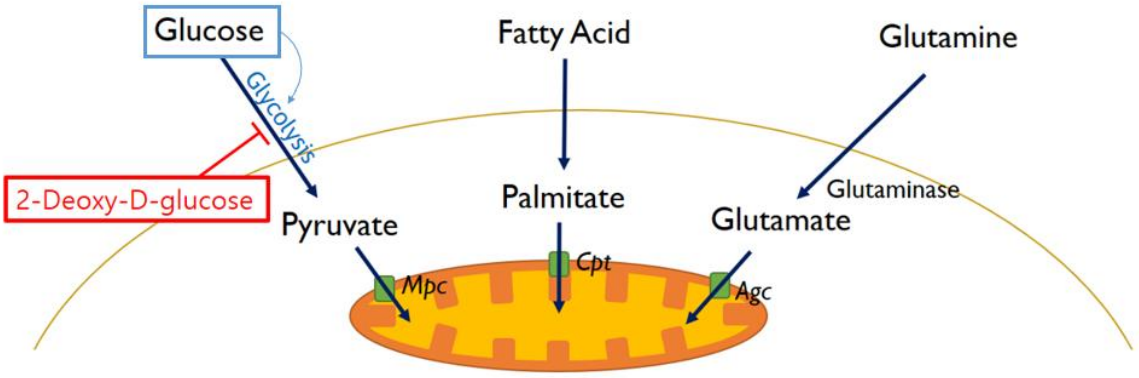

Figure 7. Adipocyte use glucose and fatty acid as energy source. Glucose metabolized by glycolysis pathway generates ATP. 2-Deoxy-D-glucose (2-DG) which has the 2-hydroxyl group replaced by hydrogen can competitively inhibit glycolysis. Mpc, mitochondria pyruvate carrier; Cpt, carnitine palmitoyltransferase; Agc, aspartate-glutamate carrier

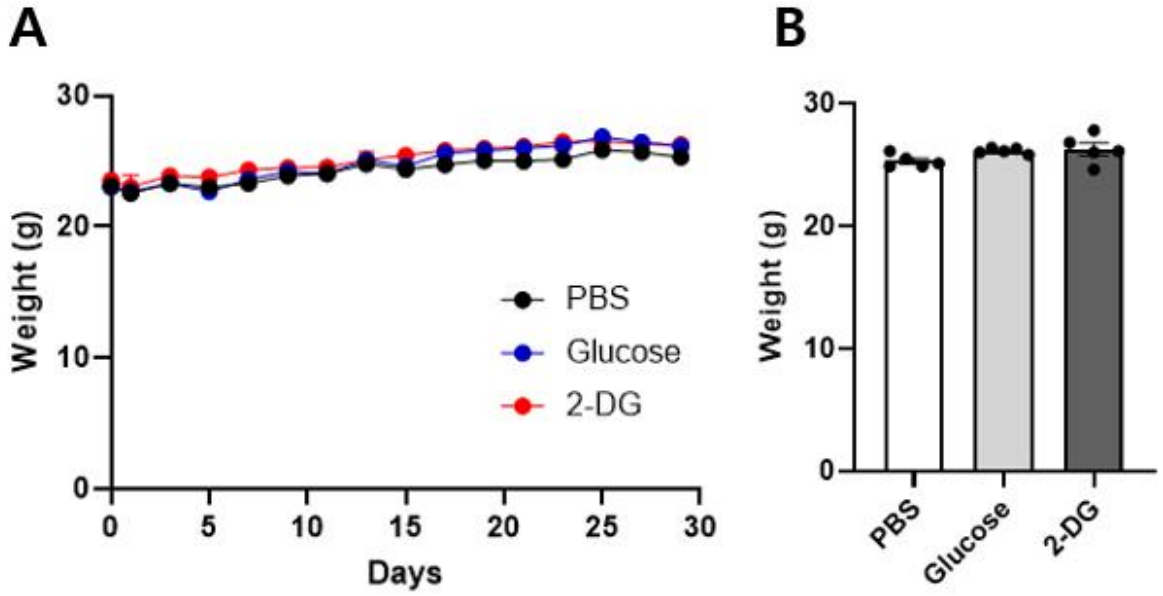

Figure 8. Localized injection in fat grafts does not affect whole-body metabolism. (A) Mouse weight tracking during the 4-week injection period (n = 5) indicated comparable weights. (B) Weights of mouse show no significant difference between three groups at the point of tissue harvest. Data are presented as means ± standard errors of the mean. PBS, phosphate-buffered saline; 2-DG, 2-Deoxy-D-glucose.

PBS group	1	2	3	4	5
Control side	0.136	0.162	0.132	0.102	0.157
Graft side	0.071	0.089	0.103	0.084	0.125
Before grafting	0.092	0.119	0.107	0.100	0.095

Glucose group	6	7	8	9	10
Control side	0.119	0.149	0.120	0.123	0.131
Graft side	0.085	0.135	0.084	0.109	0.099
Before grafting	0.117	0.119	0.088	0.077	0.112

2-DG group	11	12	13	14	15
Control side	0.109	0.175	0.132	0.119	0.104
Graft side	0.057	0.089	0.057	0.061	0.063
Before grafting	0.094	0.123	0.087	0.084	0.123

Table 2. phosphate-buffered saline (PBS) (2-DG) (A) PBS group (B) Glucose group (C) 2-DG group. Weights shown in grams (g).

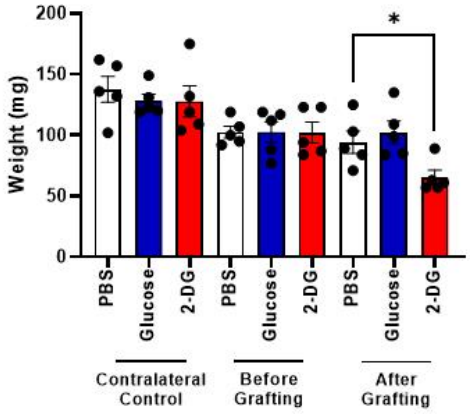

Figure 9. Glycolysis inhibition in fat grafts reduces the graft retention rate. Comparative analysis shows significant decrease in the weight of after grafting adipose tissue in 2-Deoxy-D-glucose (2-DG) group than phosphate-buffered saline (PBS) group. In glucose group, the weight of after grafting adipose tissue increased than other groups. $*p < 0.05$ between indicated group. Data are presented as means ± standard errors of the mean.

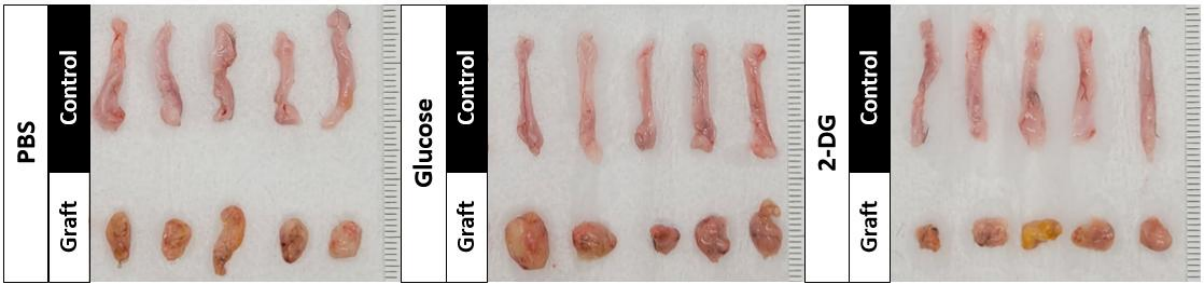

Figure 10. Pharmacological glycolysis regulation in fat grafts affects graft retention rates. Gross appearances of the 4-week phosphate-buffered saline (PBS), glucose and 2-Deoxy-D-glucose (2-DG) injected tissues after fat grafting (n = 5) show more decreased size of grafted adipose tissue in 2-DG groups.

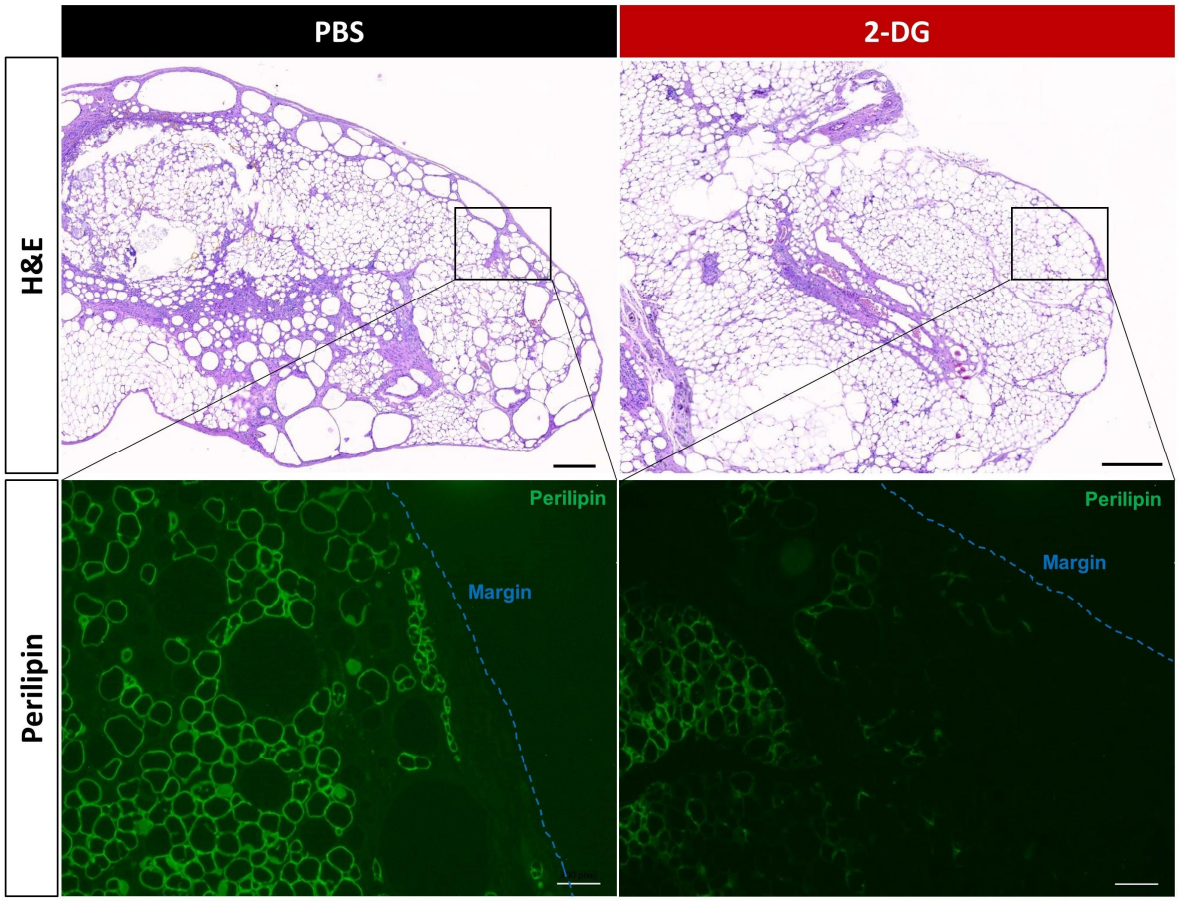

Figure 11. Glycolysis inhibition in fat grafts reduces marginal adipocyte survival. Hematoxylin and eosin (H&E) (above) and perilipin (below) staining of fat graft tissue after 4 weeks of phosphate-buffered saline (PBS) or 2-Deoxy-D-glucose (2-DG) injections. 2-DG group shows more fibrosis and lipid vacuoles with low perilipin staining than PBS group. Scale bars: 200 μm for H&E and 25 μm for perilipin staining.